

This is the peer reviewed version of the following article:

Label free detection of plant viruses with organic transistor biosensors / Berto, Marcello; Vecchi, Eugenia; Baiamonte, Luca; Condò, Carla; Sensi, Matteo; Di Lauro, Michele; Sola, Marco; De Stradis, Angelo; Biscarini, Fabio; Minafra, Angelantonio; Bortolotti, Carlo Augusto. - In: SENSORS AND ACTUATORS. B, CHEMICAL. - ISSN 0925-4005. - 281:(2019), pp. 150-156. [10.1016/j.snb.2018.10.080]

Terms of use:

The terms and conditions for the reuse of this version of the manuscript are specified in the publishing policy. For all terms of use and more information see the publisher's website.

18/12/2025 18:58

Accepted Manuscript

Title: Label free detection of plant viruses with organic transistor biosensors

Authors: Marcello Berto, Eugenia Vecchi, Luca Baiamonte, Carla Condò, Matteo Sensi, Michele Di Lauro, Marco Sola, Angelo De Stradis, Fabio Biscarini, Angelantonio Minafra, Carlo Augusto Bortolotti



PII: S0925-4005(18)31849-5
DOI: <https://doi.org/10.1016/j.snb.2018.10.080>
Reference: SNB 25514

To appear in: *Sensors and Actuators B*

Received date: 14-6-2018
Revised date: 26-9-2018
Accepted date: 14-10-2018

Please cite this article as: Berto M, Vecchi E, Baiamonte L, Condò C, Sensi M, Di Lauro M, Sola M, De Stradis A, Biscarini F, Minafra A, Bortolotti CA, Label free detection of plant viruses with organic transistor biosensors, *Sensors and amp; Actuators: B. Chemical* (2018), <https://doi.org/10.1016/j.snb.2018.10.080>

This is a PDF file of an unedited manuscript that has been accepted for publication. As a service to our customers we are providing this early version of the manuscript. The manuscript will undergo copyediting, typesetting, and review of the resulting proof before it is published in its final form. Please note that during the production process errors may be discovered which could affect the content, and all legal disclaimers that apply to the journal pertain.

Label free detection of plant viruses with organic transistor biosensors

Marcello Berto^a, Eugenia Vecchi^a, Luca Baiamonte^a, Carla Condò^a, Matteo Sensi^a, Michele Di Lauro^a, Marco Sola^a, Angelo De Stradis^b, Fabio Biscarini^{a,c}, Angelantonio Minafra^b and Carlo Augusto Bortolotti^{a*}

a. Dipartimento di Scienze della Vita, Università di Modena e Reggio Emilia, Via Campi 103, 41125 Modena, Italy

b. Consiglio Nazionale delle Ricerche, Istituto per la Protezione Sostenibile delle Piante, via Amendola 122/D, 70126 Bari, Italy

c. Istituto Italiano di Tecnologia – Center for Translational Neurophysiology, Via Fossato di Mortara 17-19, 44121 Ferrara, Italy

* Corresponding author at: Dipartimento di Scienze della Vita, Università di Modena e Reggio Emilia, Via Campi 103, 41125 Modena, Italy

E-mail address: schoening@fh-aachen.de (M.J. Schöning)

e-mail: carloaugusto.bortolotti@unimore.it (C. A. Bortolotti)

Highlights

- Plum Pox Virus affects stone fruit trees and causes severe economic damages
- The PPV biosensor is based on a Electrolyte-Gated Organic Field-Effect Transistor
- Sensitivity and dynamic range are comparable to those of commercially available platforms

Abstract

Plum Pox Virus (PPV) is the pathogen responsible for Sharka, a highly infectious disease affecting stone fruit trees and causing severe economic damages, which can be only contained through early-detection and frequent monitoring. We propose a bioelectronic PPV biosensor, based on a electrolyte-gated organic field-effect transistor (EGOFET), for the specific detection of PPV in plant extracts with a sub ng/ml detection limit. The sensing unit of the biosensor is based on anti-PPV antibodies, uniformly oriented on the gold gate electrode by using a sub-monolayer of Protein G. The sensitivity and dynamic range of the EGOFET-based biosensor are comparable to those of commercially available platforms for detection of plant pathogens. This novel electronic immunosensor is compatible with low-cost fabrication procedures and can be easily reconfigured into a fully portable device to be operated in greenhouse and in the field orchards.

Keywords: Plum Pox Virus; Sharka; EGOFET; Organic Bioelectronics

Introduction

Plant pathogens represent a major danger affecting the agricultural productivity: crop losses due to plant infections cause severe economic damages and jeopardize the sustainability of the increasing food demand worldwide.[1–3] The main plant pathogens include fungi, bacteria and viruses; among viral diseases of plants, Sharka is definitely one of most devastating and worldwide-spread. Sharka affects plants belonging to the *Prunus* genus, including peach, cherry, plum, and apricot.[4] While crop losses typically range between 20% and 40%, [5] in some cases Sharka affected cultivars can reach even 100% losses.[6,7] The economic burden associated with plant infections is not solely related to yield losses and decreased fruit quality: high costs associated to preventing, diagnosing and managing the disease, through quarantine and eradication, should also be taken into account.[7] The symptoms of Sharka, detectable at

a visual inspection, appear several months after the infection, and the only measure to limit damages to the production is the plant elimination: these considerations generate a strong need for highly sensitive methods for early detection of this pest in symptomless plants.

The causative agent of Sharka is *Plum pox virus* (PPV). This flexuous-shaped virus, with a single stranded polycistronic RNA genome of ca. 9kb, consists of several strains showing different features in diffusion and virulence on the different *Prunus* hosts.[4] It is efficiently transmissible by aphid vectors in a semi-persistent manner. Long distance diffusion is operated by human trade of infected plant vegetative material (budwood and rootstocks). The erratic presence of the virus inside mature tree branches and a relative low titer in woody tissues[8] makes sometimes still difficult the correct diagnosis of the infected plants even through advanced molecular tools.[9] The EU quarantine regulations (Directive 2000/29) ask for mandatory controls either for the declared new foci monitoring as well as on the post-entry consignments of *Prunus* plants for planting. In this perspective, the availability of a quick, inexpensive and sensitive diagnostic tool to screen even dormant propagative material is highly desirable.

The two main families of biosensing methods for plant viruses are immunoassays and the so-called molecular detection methods:[10] techniques belonging to the first group are based on the use of antibodies specific to the pathogen antigens and include enzyme-linked immunosorbent assay (ELISA), immunoblotting and lateral flow (LF), although novel approaches, e.g. based on immunochromatography[11] or Electrochemical impedance Spectroscopy (EIS),[12,13] have been recently demonstrated. On the contrary, the molecular methods are based on the detection of nucleic acids, with real time RT-PCR offering the best performances in terms of sensitivity and accuracy but suffering of lack of portability that hinders in-field deployment.[3]

Organic electronic based devices are emerging as novel players in the field of biosensing, both in the Electrolyte Gated Organic Field Effect Transistor (EGOFET) and Organic Electrochemical Transistor (OECT) configurations.[14–20] They offer a unique set of advantages deriving both from the use of organic electronic materials (guaranteeing low production costs in environmental friendly conditions and on flexible substrates) and on their working principle, which exploits the intrinsic amplification offered by FET to endow them with tremendously low limit of detection[21–24] and operational voltages well below 1V. EGOFET and OECT immunobiosensors require the immobilization of a bioreceptor at one of the relevant device interfaces. Here, we present an EGOFET-based biosensor for the quantification of Plum pox virus in plant extracts. Our sensing strategy is based on the

immobilization of anti-PPV polyclonal antibodies (Abs) on the gate electrode with controlled orientation: incubation of the gate with suspensions containing PPV leads to specific binding of the latter to the electrode surface and the Ab-virus interaction is transduced into an electric signal proportional to the PPV levels in the sample. The response is label-free, rapid and specific. To the best of our knowledge, this is the first example of virus detection with an electronic sensor based on an organic transistor architecture, and the first report of quantitative detection of a plant pathogen with an organic electronic device.

Results and discussion

Interface characterization

EGOFETs can be endowed with immunorecognition upon functionalization of surfaces located at one of their relevant interfaces. Typically, recognition moieties are immobilized either at the gate/electrolyte or at the OSC/electrolyte interface.[14,17,25–28] We opted for the former strategy, which allowed us to exploit facile thiol-gold chemistry.

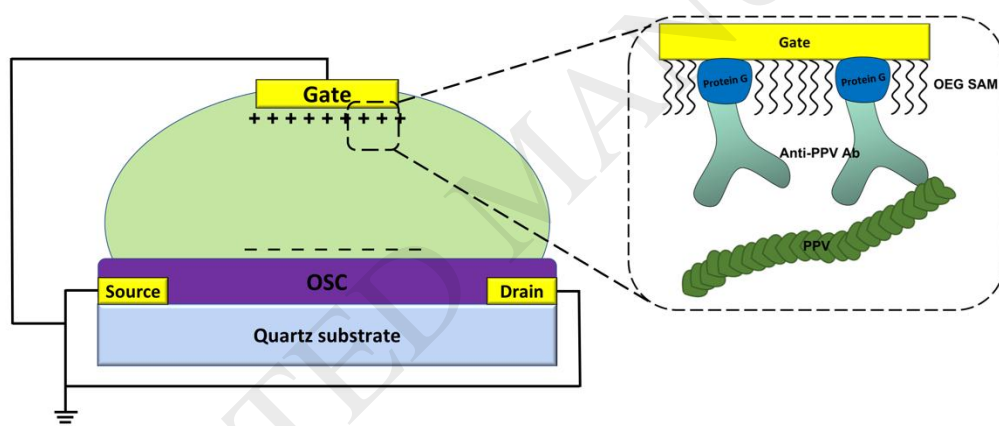


Fig. 1. Schematic experimental setup in which are highlighted source, drain, and gate electrodes, the organic semiconductor layer on the quartz substrate, the electrolyte and the electrical connections (left). On the right a zoom on the functionalization strategy: PPV antibodies are immobilized on the gate surface through covalent binding of protein G exploiting a single surface exposed Cysteine. An OEG SAM is the deposited to passivate bare gold spot eventually left on the gate surface. Neither the experimental setup nor the functionalization scheme are to scale.

In order to impart a uniform orientation to the anti-PPV Abs on the gate electrode and maximize the chance of binding events to the PPV capsid, we first deposited a (sub)monolayer of recombinant Protein G onto the surface as previously described.[17] Protein G has high affinity for the heavy chain of Immunoglobulins G,[29–31] and therefore serves as a primer to further graft the antibody on the surface with a precise, uniform orientation. At variance with previous works,[17,18,32] Protein G was covalently bound to the Au exploiting a single surface exposed engineered Cys residue[33] (see Experimental section for details). Following

Protein G immobilization and subsequent anti-PPV Abs adsorption, we deposited a (11-Mercaptoundecyl)tri(ethylene glycol), OEG, self-assembled monolayer to avoid non-specific adsorption to the gold surface spots not covered by the ProteinG/Ab construct (Figure 1).

The stepwise functionalization strategy was monitored by cyclic voltammetry as shown in Figure 2, where cyclic voltammograms recorded at different functionalization steps in a 5 mM solution of $[\text{Fe}(\text{CN})_6]^{3-/4-}$ are shown. The Protein G chemisorption causes an increase of the peak-to-peak distance and a decrease of the current density, as expected for partial (albeit not total) surface derivatization that hinders the accessibility of the redox probe to the surface. The Ab immobilization basically leaves the CV curves unchanged, since anti-PPV Abs tend to bind to chemisorbed Protein G sites, thus not affecting the overall surface coverage. Final functionalization with the OEG SAM completely inhibits the faradic response, an indication that no bare spots are left on the gate surface. From these measurements, one can estimate by means of the Randles-Sevcick equation the coverage of the electrode by Protein G/Ab to be $42(\pm 2) \%$ (see Experimental section).

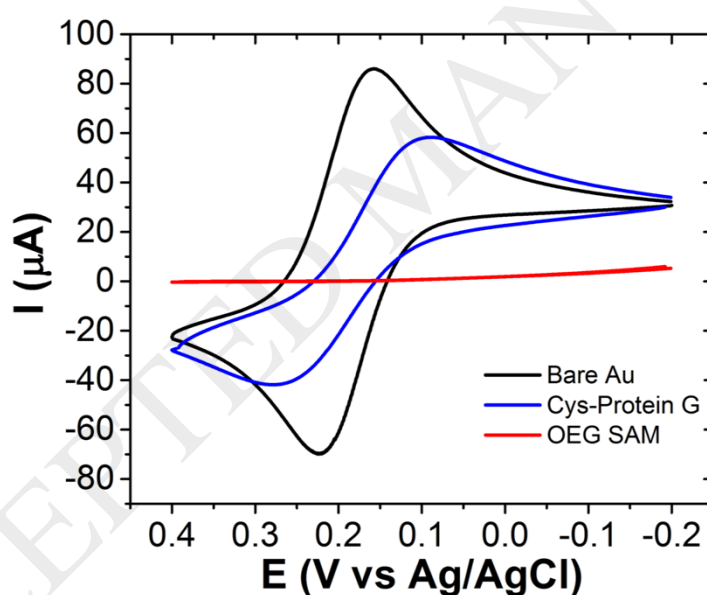


Fig. 2. Cyclic voltammograms obtained with the Gate electrode at different functionalization steps: bare Au electrode (black), after functionalization with Cys-Protein G (blue) and after passivation with OEG SAM (red).

The capability of the EGOFET to selectively detect the presence of PPV virions was assessed by incubating the functionalized gate ex situ, in solutions containing increasing [PPV]. The EGOFET transfer characteristics were recorded in phosphate buffer saline (PBS) 50 mM, pH 7.4 at $V_{\text{DS}} = -0.2 \text{ V}$, and the transistor parameters extracted in the linear regime, in line with previous works of our group.[32,34] Figure 3a displays the overlay of transfer characteristics obtained after exposure of the functionalized gate electrode: as [PPV] increases, it can be observed a decrease of the current I_{DS} and a decrease of the slope of the linear region of the

transfer curves. To construct a quantitative dose curve of the EGOFET biosensor, we define the device response as the relative current variation (at $V_{GS} = -0.7$ V) normalized to the blank response (viz. $[PPV]=0$). The corresponding dose curve is reported in Figure 3b.

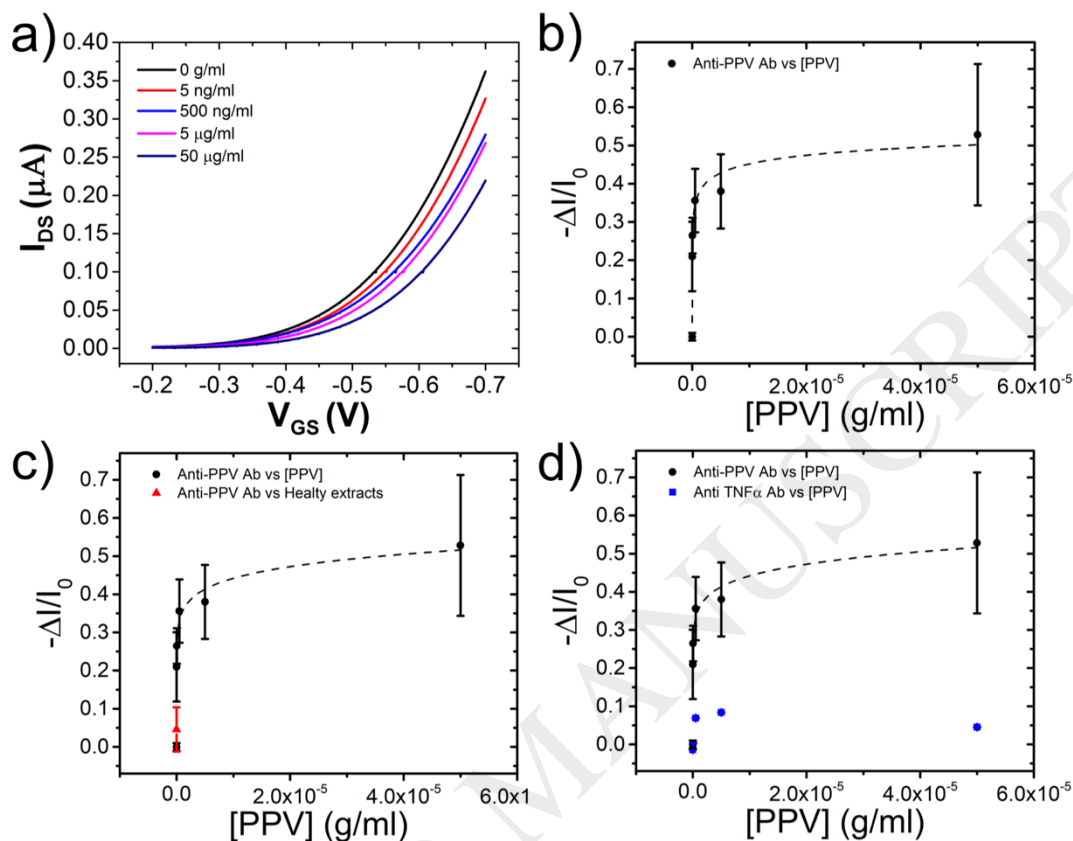


Fig. 3. a) Transfer characteristics of the sensor resulting from exposure to different [PPV] solutions (concentrations are reported in the legend). b) Biosensors dose curve $-\Delta I/I_0$ vs [PPV]. Control experiments: c) normalized I_{DS} current response versus [PPV] (black markers) compared with the sensor response in PPV-free solution from healthy plant extract (red triangle) and d) for gate functionalized with aspecific anti-TNF α antibody (blue squares). The dashed black line is only a guide for the eye.

The I_{DS} current decreases with increasing concentration of PPV. The binding event occurring at the surface leads to modifications on different length and timescales, and might cause conformational changes of the receptor, charge rearrangements, reorganization of the water molecules at the interface. Because of the strong capacitive coupling between the gating system and the semiconductor channel, even small capacitance changes occurring at the biorecognition layer will be amplified into detectable variations of the EGOFET parameters.[14,35,36] Indeed, EGOFET are multi-parametric devices, meaning that different figures of merit can vary in response to binding events between a surface-immobilized receptor (here, the anti-PPV Ab) and its partner in solution (in our case, the PPV molecules). One can monitor variations of the drain current I_{DS} as a function of the analyte concentration;[18,27,32,34,37] in several cases, the main consequence of the binding between the two partners is a change in the threshold voltage V_{th} , [23,24,36] the minimum gate voltage

needed to induce the conducting channel between source and drain. Nevertheless, the transconductance g_m , i.e. the slope of the transfer curve, the electrical parameter relating the variation of the output current to the input voltage (which embodies the product of the charge mobility μ and the capacitance C) is frequently observed to change upon binding. Attempts have been made to rationalize what figures of merit should vary in response to different molecular interaction.[19,24,35] Nevertheless, due to the complex nature of the biomolecular interaction event and the lack of an operational model for EGOFETs, an unambiguous assignment of what are the phenomena behind the variation of I_{DS} , V_{th} , g_m from a molecular perspective is still challenging. In the present case, visual inspection of Figure 3a seems to indicate that the main changes induced in the device response by the binding of PPV to the gate surface can be ascribed to changes in the transconductance g_m , with minor repercussion on the threshold voltage V_{th} .

This is confirmed by the plots in Figure 4b and 4c. The g_m is affected by PPV concentration and follows a trend qualitatively similar to that of $\Delta I/I_0$, but the V_{th} change is rather small in magnitude (about 30 mV when switching from a virus-free solution to one containing 50 $\mu\text{g/l}$ PPV). It could be noticed that the large error affecting the extrapolated V_{th} values makes

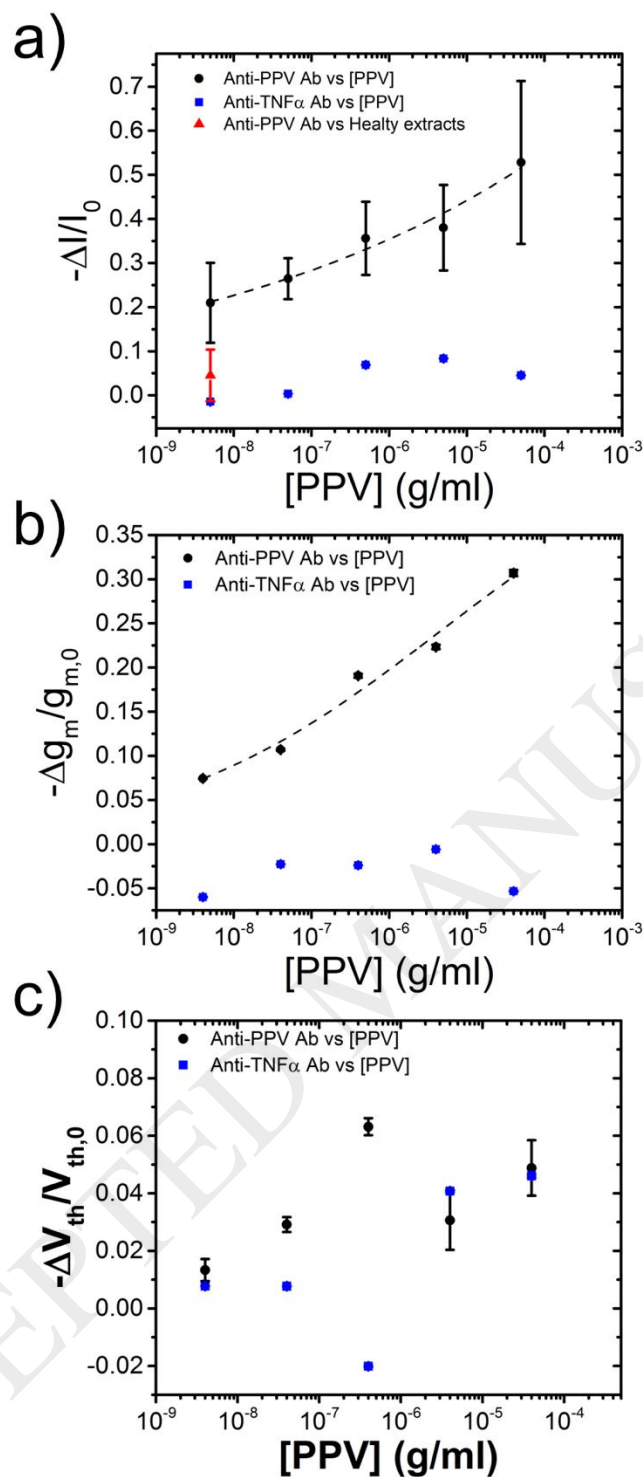


Fig. 4. a) Relative variation of current response acquired at $V_{GS} = -0.7$ V as function of [PPV] (black circles), sensor behaviour in PPV-free sample (red triangle) and comparison with Anti-TNF α antibodies functionalized sensor (blue squares). b) Relative variation of EGO-FET-sensor transconductance g_m and c) threshold voltage V_{th} as function of [PPV] (black circles). The dashed black lines are a guide for the eye.

difficult to assess its trend on safe grounds. Conversely, the normalized variation of transconductance (i.e. the changes in the transconductance at different PPV concentrations, divided by the transconductance value obtained in a PPV-free solution), is a strategy to minimize device-to-device variations.[38] A marked monotonic variation of $-\Delta g_m/g_{m,0}$ on the PPV concentration which follows a logarithmic increase up to [PPV] = 5 μ g/ml is apparent.

In the present case, the changes of g_m seem to be the most robust parameter to quantify the PPV levels in the samples.

We then rationalize the response using the simplest arguments based on capacitive coupling in the EGOFET. As the functionalization takes place on the gate, we assume that the mobility μ of the semiconductor is unaffected by the PPV binding and can be considered as constant.[35] The changes in g_m can therefore be assigned to modification of the gating capacitance upon biorecognition of PPV by its antibody: the decrease of capacitance that we observe upon binding can be detected thanks to the total passivation of the gate electrode, as indicated by electrochemical characterization. This is in line with previously described EGOFET-based biosensors with fully passivated functionalized gate,[19,27] and yields the conclusion that in the present case the biosensor response is capacitance-modulated: $\Delta I/I_0$ is dominated by changes in C (with the capacitance at the Ab/PPV interface contributing the most to the overall capacitance) rather than by threshold voltage variations. The effect of the stepwise gate functionalization procedure, and in particular of the binding of PPV to gate-immobilized antibodies, on the gate electrode capacitance was further confirmed by Electrochemical Impedance Spectroscopy (EIS) investigations (see Figures S1 and S2).

From the dose curve in Figure 3b, we estimated the theoretical LOD (see Methods section) to be 180 pg/ml. As a blank, we used a diluted healthy (i.e. PPV-free) plant extract (see Control experiments section below). The actual concentration range detected spanned four orders of magnitude, ranging from 5 ng/ml to 50 μ g/ml. Although the LOD of our EGOFET is about one order of magnitude higher than that of Electrochemical Impedance Spectroscopy (EIS)-based PPV detection,[13] the EGOFET response dynamic range is two orders of magnitude larger. Most importantly, the EGOFET-based immunosensor presented here shows higher sensitivity than the currently used, commercially available serological techniques (like ELISA-based approaches and commercial rapid immunocromatographic assays) whose LODs lie in the ng/ml range.

A further step of analysis, beyond the successful proof of concept we present in this paper, will be done with untreated/raw sap of healthy and infected plants (also natural woody hosts) and in a time course of infection progress. Final aim is to deploy a detection tool suitable for in-field analysis.

Control experiments

To unambiguously assess that the change in the electrical parameters of the EGOFET could be safely ascribed to specific binding of PPV to its corresponding Ab immobilized at the gate electrode, we performed the following control experiments. We first exposed the gate

electrode functionalized with Protein G followed by immobilization with anti-PPV Ab, to extracts derived from healthy tobacco leaves. The samples were prepared exactly as described for those containing the PPV (i.e. by diluting leaves extracts in PBS at different ratios), with the only exception that the tobacco leaves belonged to plants that have not been infected by PPV. We then recorded transfer characteristics upon ex situ incubation of the gate with such healthy control extracts. Neither the normalized current (red triangle in Figure 3c and Figure 4a) nor the normalized transconductance responses (data not shown) exhibited a monotonic trend with increasing amount of plant-derived material (proteins, nucleic acids, small chemicals) in the samples, and for all the investigated dilutions the changes in I_{DS} or g_m was negligible with respect to what is observed in the presence of PPV at the lowest concentration.

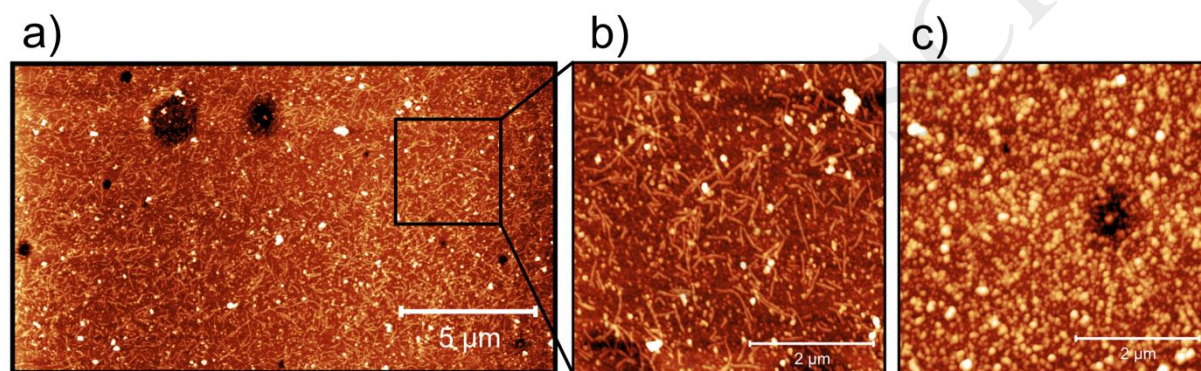


Fig. 5. a) Semi-contact mode AFM morphological images of PPV immobilized on gold functionalized with anti-PPV Ab; b) magnification of a region of panel a; c) Control experiment: bare gold electrode after immersion in a PPV solution ([PPV] = 50 $\mu\text{g/ml}$ in PBS 50mM, pH 7.4).

A second control experiment was performed by functionalizing the gate with Protein G and a different Ab: we used an anti-Tumor Necrosis Factor ($\text{TNF}\alpha$) Ab, which is not specific to PPV and was therefore not expected to bind the virus (see Figure 3d). The ProteinG-AntiAb gate was exposed to solutions containing different PPV concentrations: the corresponding extracted current and transconductance relative variation are displayed in Figure 4a and 4b, respectively. No significant change in the performances of the device could be observed, indirectly indicating that the current changes observed in Figure 4a and depicted as black circles are mostly to be ascribed to specific Ab-PPV interactions.

Finally, we checked by means of Atomic Force Microscopy the immobilization of PPV virions on a functionalized Au film. The Au substrates were functionalized with the same procedure for gate electrodes and incubated in a 50 $\mu\text{g/ml}$ PPV-containing suspension in PBS 50mM, pH 7.4. The AFM images in Figure 5 were acquired operating the AFM in air. The elongated features in Figure 5a and 5b correspond with the shape and size expected for PPV particles (approximately 500-700 nm in length and 15-20 nm in width), [4,39] and therefore provide a

further evidence of the efficacy of the functionalization strategy to bind the virions. As a negative control, bare gold was also exposed to a 50 µg/ml solution of PPV (see Figure 5c): no PPV can be detected on the non-functionalized surface.

Conclusions

In this work, we demonstrated an organic electronics-based biosensor for the specific detection of PPV in partially purified plant extracts. The biosensor is based on the EGO-FET architecture and its sensing unit is a gold gate electrode functionalized with anti-PPV polyclonal antibodies (as purified IgGs). Upon binding of the PPV to the surface immobilized antibody, we observe changes in the drain current mainly due to changes in transconductance, while the threshold voltage is only minimally affected by the biorecognition. This finding suggests that the biosensor response is dominated by changes in capacitance. By constructing a calibration curve based on transconductance changes as a function of PPV concentration, we could estimate a theoretical LOD of 180 pg/ml and operate the biosensor within a dynamic range spanning four orders of magnitude, from 5 ng/ml to 50 µg/ml. Our devices provide a label free and rapid response, with high selectivity (as confirmed by negative control experiments) and sensitivity comparable to that of ELISA platforms. Our results therefore provide a proof of concept that organic bioelectronics devices can be successfully applied to the detection of plant pathogens, challenging the state-of-the-art platforms currently available. The further steps to be taken will concern the optimization of the device architecture, possibly also including tailor-made microfluidics, to perform measurements directly on the untreated (raw) plant sap.

Experimental Section

Virus preparation and polyclonal antibodies

PPV (M strain)[40] was maintained in *Nicotiana benthamiana* plants upon periodical mechanical inoculation. Virus particles partial purification was performed as in reference 40 with modification. At 15 days post-inoculation, *ca.* 90 grams of leaves from infected or healthy plants (used as negative control) were homogenized in ice-cold Tris-HCl buffer (0.1 M pH 8.0, added of 0.3% Na metabisulfite). The filtered slurry was mixed with 1/3 vol of chloroform-butanol (1:1 mixture) by stirring on ice for 30'. To the supernatant obtained after a low speed centrifugation (8k rpm for 20'), 8% polyethylene glycol (PEG 8000) and 1% NaCl were added to precipitate the virus particles for 1h on ice. The suspension is centrifuged at 12k rpm for 20' and the pellet resuspended overnight in cold with a small volume of Tris-

HCl buffer 10 mM. After a short low speed centrifugation to remove all the residual green material, a high speed centrifugation (40k rpm for 2h) on a 30% sucrose cushion is done. The final pellet is resuspended in 1 ml of Tris buffer and OD red on NanoDrop (ThermoFisher). Assuming for PPV particles an extinction coefficient (A_{260}) of about 3.0,[41] the final virus yield was 0.77 mg/ml.

Polyclonal antibodies, raised in rabbit against purified PPV, were kindly supplied by *AgriTest* srl (Valenzano, Italy). The purified IgGs, obtained after a protein A-Sepharose step on healthy *N. benthamiana* sap pre-absorbed antiserum, are concentrated at 1mg/ml suspension and kept always at -20°C.

Device Fabrication

The Test Patterns (TPs) featuring 4 interdigitated electrodes with channel length $L = 15 \mu\text{m}$ and channel width $W = 30 \text{ nm}$ ($W/L = 2000$) patterned by photolithography and lift-off (1 cm^2 total area) were purchased from “Fondazione Bruno Kessler” (FBK, Trento, Italy). Source and Drain electrodes are made of Au 50 nm thick with a few nm of Cr adhesive layer on a quartz substrate, with a roughness lower than 2 nm. TPs were cleaned following the procedure: (i) a rinse with acetone (10 ml) to remove the photoresist layer, (ii) drying gently with nitrogen flow, (iii) washing again in hot acetone for 15 min, and (iv) drying with nitrogen. A final rinse with water was done before the semiconductor deposition. Pentacene was deposited by thermal sublimation in high vacuum on substrates held at RT (base pressure 10^{-8} mbar, rate $2.5 \text{ \AA}/\text{min}$). The pentacene film was 15 nm (10 monolayers) for all samples.

Gate functionalization

The polycrystalline Au wire gate electrode (GE) was cleaned as follows: flaming it in oxidizing conditions, immersion in hot KOH for 4h, rinse with abundant water and immersion in hot concentrated H_2SO_4 for 2 h. The electrode was then cycled 20 times between +1.5 and -0.25 V at 0.1 V s^{-1} in 1 M H_2SO_4 .

Gold GE was functionalized according to the following immobilization protocol: (i) a first incubation in a phosphate buffer saline (PBS 50 mM, pH 7.4) of Cys-Protein G (2 mg/ml) for 4h at room temperature (RT), (ii) a rinse with PBS, (iii) incubation with an anti-PPV (0.1 mg/ml) solution for 1 h at RT (iv) a rinse with PBS, (v) immersion in OEG thiol 100 μM (in PBS 50 mM, pH 7.4) for 20 minutes and (vi) a final rinse with PBS.

Electrochemical characterization

Cyclic voltammetry (CV) experiments were performed to estimate the electrode active area and the coverage after cys-PG immobilization and OEG SAM formation by means of the Randles-Sevcik equation (Figure 2).

The method consists of monitoring the cathodic current, corresponding to the $[\text{Fe}(\text{CN})_6]^{3-}$ reduction, as a function of the incubation time of the working electrode. In particular, protein G binding the gold surface, causes an increase of the passivation of the electrode, seen by the decrease of the faradaic current. We then use the Randles–Sevcik equation to extract variation in the electrode active area. The measurements were performed in 1 M KCl and 5 mM $\text{K}_3[\text{Fe}(\text{CN})_6]^{3-}$ at 20 mV s^{-1} . Impedance spectra shown in Fig S1, Supporting Informations, were performed in 0.1 M PBS and 0.5 mM $\text{K}_3[\text{Fe}(\text{CN})_6]^{3-}$ (Faradaic) and in 0.05 M PBS (non-Faradaic), at an initial potential of 0.17 V and in a frequency range from 0.1 Hz to 10 KHz. The gate was functionalized as previously described.

A CH Instrument potentiostat 760c model was used for the cyclic voltammetry (CV) experiments and the Electrochemical Impedance Spectroscopy (EIS), which were carried out using a three-electrode cell. The GE was used as a working electrode (WE), whereas a Pt wire and a Ag/AgCl electrode (Elbitech, Livorno Italy) were chosen as counter electrode (CE) and reference electrode (RE), respectively. The gold WE was cleaned as described above in the text.

Electrical Characterization

Electrical measurements were acquired in a buffer solution (PBS 50 mM, pH 7.4) confined in a PDMS pool. Source, drain, and gate electrodes were connected to an Agilent B2902A Source Meter Unit. All measurements were carried out at room temperature. Gate electrode was incubated *ex situ* in solutions containing increasing [PPV] before electrical measurements for 15 minutes, in line with literature data. Gate electrode area was kept constant by means of a passivation layer.

The I–V transfer characteristics were performed by sweeping the gate-source voltage (V_{GS}) from +0.2 to –0.5 V while leaving the drain-source voltage (V_{DS}) constant at –0.2 V (linear regime), in line with previous works from our group.

We calculated the limit of detection (LOD) as the mean value of the blank +3 times its corresponding standard deviation, using the responses of the negative controls as blank responses.[42]

Atomic Force Microscopy

Gate electrodes morphology was characterized by means of an NT-MDT SMENA Solver platform (Moscow, Russia); all images were obtained in air in semi-contact mode and analyzed using Gwyddion 2.48 freeware (<http://gwyddion.net>).

The electrodes used for AFM characterization are different from the one used for electrical measurements. We used a flat silicon chip covered by 50 nm of Au, the fabrication of which is described elsewhere,[18] in order to optimize the morphological analysis.

Chemicals & Reagents

Phosphate salts, potassium ferricyanide, potassium chloride, sulfuric acid, potassium hydroxide, acetone, OEG SAM, tris(hydroxymethyl)aminomethane, PEG and pentacene were purchased from Sigma-Aldrich. Cys-Protein G was purchased from Space Import-Export s.r.l. (Milano, Italy).

Conflicts of interest

“There are no conflicts to declare”.

Acknowledgements

CAB acknowledges the “Fondazione di Vignola” and Life Science Department through “FAR2017” for support.

Authors wish to thank Dr V. Elicio (www.agritest.it) for the kind supply of purified anti-PPV IgG from polyclonal antiserum.

References

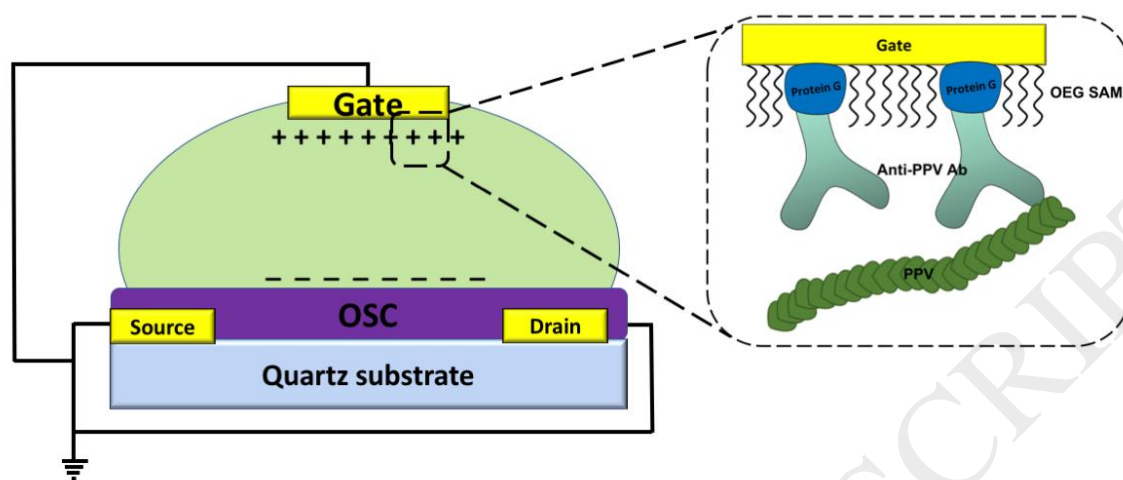
- [1] S. Sankaran, A. Mishra, R. Ehsani, C. Davis, A review of advanced techniques for detecting plant diseases, *Comput. Electron. Agric.* 72 (2010) 1–13. doi:10.1016/j.compag.2010.02.007.
- [2] P. Narayanasamy, *Microbial Plant Pathogens-Detection and Disease Diagnosis*, Springer Netherlands, Dordrecht, 2011. doi:10.1007/978-90-481-9769-9.
- [3] M. Khater, A. de la Escosura-Muñiz, A. Merkoçi, Biosensors for plant pathogen detection, *Biosens. Bioelectron.* 93 (2017) 72–86. doi:10.1016/j.bios.2016.09.091.
- [4] J. Sochor, P. Babula, V. Adam, B. Krska, R. Kizek, Sharka: The past, the present and the future, *Viruses*. 4 (2012) 2853–2901. doi:10.3390/v4112853.
- [5] Y. Fang, R.P. Ramasamy, Current and prospective methods for plant disease detection, *Biosensors*. 5 (2015) 537–561. doi:10.3390/bios5030537.
- [6] M. Cambra, N. Capote, A. Myrta, G. Llácer, Plum pox virus and the estimated costs associated with sharka disease, *EPPO Bull.* 36 (2006) 202–204. doi:10.1111/j.1365-2338.2006.01027.x.
- [7] J.A. García, M. Glasa, M. Cambra, T. Candresse, Plum pox virus and sharka: A model potyvirus and a major disease, *Mol. Plant Pathol.* 15 (2014) 226–241. doi:10.1111/mpp.12083.
- [8] EPPO, Plum pox potyvirus, *EPPO Bull.* 34 (2004) 247–256. doi:10.1111/j.1365-2338.2004.00726.x.
- [9] A. Olmos, E. Bertolini, M. Gil, M. Cambra, Real-time assay for quantitative detection of non-persistently transmitted Plum pox virus RNA targets in single aphids, *J. Virol. Methods*. 128 (2005) 151–155. doi:10.1016/j.jviromet.2005.05.011.
- [10] M.J. Clemente-Moreno, J.A. Hernández, P. Diaz-Vivancos, Sharka: How do plants respond to Plum pox virus infection?, *J. Exp. Bot.* 66 (2015) 25–35. doi:10.1093/jxb/eru428.
- [11] K. Maejima, M. Himeno, O. Netsu, K. Ishikawa, T. Yoshida, N. Fujita, M. Hashimoto, K. Komatsu, Y. Yamaji, S. Namba, Development of an on-site plum pox virus detection kit based on immunochromatography, *J. Gen. Plant Pathol.* 80 (2014) 176–183. doi:10.1007/s10327-014-0504-8.
- [12] M. Ambrico, P.F. Ambrico, A. Minafra, A. De Stradis, D. Vona, S.R. Cicco, F. Palumbo, P. Favia, T. Ligonzo, Highly Sensitive and Practical Detection of Plant Viruses via Electrical Impedance of Droplets on Textured Silicon-Based Devices, *Sensors*. 16 (2016) 1946. doi:10.3390/s16111946.
- [13] U. Jarocka, M. Wasowicz, H. Radecka, T. Malinowski, L. Michalczuk, J. Radecki, Impedimetric immunosensor for detection of plum pox virus in plant extracts, *Electroanalysis*. 23 (2011) 2197–2204. doi:10.1002/elan.201100152.
- [14] D. Wang, V. Noël, B. Piro, Electrolytic Gated Organic Field-Effect Transistors for Application in Biosensors—A Review, *Electronics*. 5 (2016) 9. doi:10.3390/electronics5010009.

- [15] X. Strakosas, M. Bongo, R.M. Owens, The organic electrochemical transistor for biological applications, *J. Appl. Polym. Sci.* 132 (2015) 1–14. doi:10.1002/app.41735.
- [16] J. Rivnay, S. Inal, A. Salleo, R.M. Owens, M. Berggren, G.G. Malliaras, Organic electrochemical transistors, *Nat. Rev. Mater.* 3 (2018) 17086. doi:10.1038/natrevmats.2017.86.
- [17] S. Casalini, A.C. Dumitru, F. Leonardi, C.A. Bortolotti, E.T. Herruzo, A. Campana, R.F. de Oliveira, T. Cramer, R. Garcia, F. Biscarini, Multiscale Sensing of Antibody–Antigen Interactions by Organic Transistors and Single-Molecule Force Spectroscopy, *ACS Nano*. 9 (2015) 5051–5062. doi:10.1021/acsnano.5b00136.
- [18] M. Berto, S. Casalini, M. Di Lauro, S.L. Marasso, M. Cocuzza, D. Perrone, M. Pinti, A. Cossarizza, C.F. Pirri, D.T. Simon, M. Berggren, F. Zerbetto, C.A. Bortolotti, F. Biscarini, Biorecognition in Organic Field Effect Transistors Biosensors: The Role of the Density of States of the Organic Semiconductor, *Anal. Chem.* 88 (2016) 12330–12338. doi:10.1021/acs.analchem.6b03522.
- [19] K. Manoli, M. Magliulo, M.Y. Mulla, M. Singh, L. Sabbatini, G. Palazzo, L. Torsi, Printable Bioelectronics To Investigate Functional Biological Interfaces, *Angew. Chemie Int. Ed.* 54 (2015) 12562–12576. doi:10.1002/anie.201502615.
- [20] D.T. Simon, E.O. Gabrielsson, K. Tybrandt, M. Berggren, Organic Bioelectronics: Bridging the Signaling Gap between Biology and Technology, *Chem. Rev.* 116 (2016) 13009–13041. doi:10.1021/acs.chemrev.6b00146.
- [21] L. Kergoat, B. Piro, M. Berggren, G. Horowitz, M.-C. Pham, Advances in organic transistor-based biosensors: from organic electrochemical transistors to electrolyte-gated organic field-effect transistors, *Anal. Bioanal. Chem.* 402 (2012) 1813–1826. doi:10.1007/s00216-011-5363-y.
- [22] M. Magliulo, A. Mallardi, R. Gristina, F. Ridi, L. Sabbatini, N. Cioffi, G. Palazzo, L. Torsi, Part per Trillion Label-Free Electronic Bioanalytical Detection, *Anal. Chem.* 85 (2013) 3849–3857. doi:10.1021/ac302702n.
- [23] S. Lai, M. Barbaro, A. Bonfiglio, Tailoring the sensing performances of an OFET-based biosensor, *Sensors Actuators B Chem.* 233 (2016) 314–319. doi:10.1016/j.snb.2016.04.095.
- [24] P. Seshadri, K. Manoli, N. Schneiderhan-Marra, U. Anthes, P. Wierchowicz, K. Bonrad, C. Di Franco, L. Torsi, Low-picomolar, label-free prolactin analytical detection with an electrolyte-gated organic field-effect transistor based electronic immunosensor, *Biosens. Bioelectron.* 104 (2017) 113–119. doi:10.1016/j.bios.2017.12.041.
- [25] F. Buth, A. Donner, M. Sachsenhauser, M. Stutzmann, J.A. Garrido, Biofunctional electrolyte-gated organic field-effect transistors, *Adv. Mater.* 24 (2012) 4511–4517. doi:10.1002/adma.201201841.
- [26] G. Palazzo, D. De Tullio, M. Magliulo, A. Mallardi, F. Intranuovo, M.Y. Mulla, P. Favia, I. Vikholm-

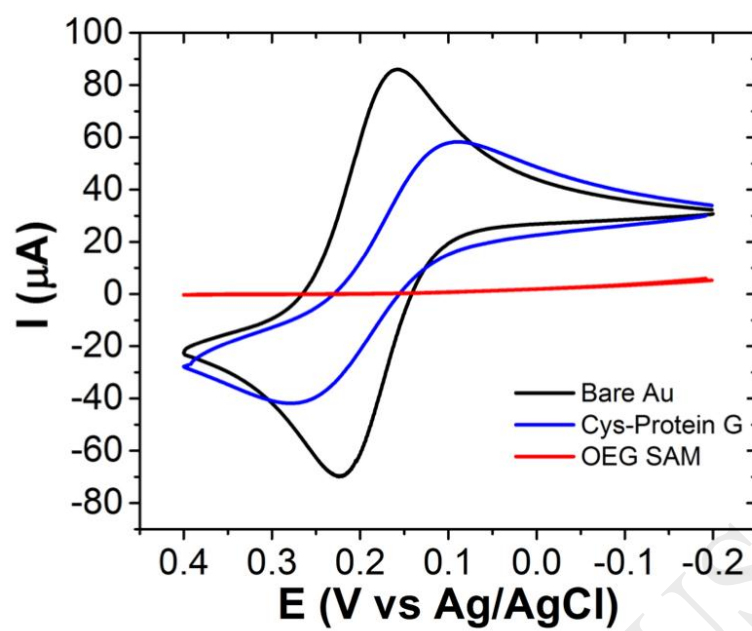
- Lundin, L. Torsi, Detection Beyond Debye's Length with an Electrolyte-Gated Organic Field-Effect Transistor, *Adv. Mater.* 27 (2015) 911–916. doi:10.1002/adma.201403541.
- [27] M.Y. Mulla, E. Tuccori, M. Magliulo, G. Lattanzi, G. Palazzo, K. Persaud, L. Torsi, Capacitance-modulated transistor detects odorant binding protein chiral interactions, *Nat. Commun.* 6 (2015) 6010. doi:10.1038/ncomms7010.
- [28] M. Larisika, C. Kotlowski, C. Steininger, R. Mastrogiacomo, P. Pelosi, S. Schütz, S.F. Peteu, C. Kleber, C. Reiner-Rozman, C. Nowak, W. Knoll, Electronic Olfactory Sensor Based on *A. mellifera* Odorant-Binding Protein 14 on a Reduced Graphene Oxide Field-Effect Transistor, *Angew. Chemie Int. Ed.* 54 (2015) 13245–13248. doi:10.1002/anie.201505712.
- [29] A.E. Sauer-Eriksson, G.J. Kleywegt, M. Uhlén, T.A. Jones, Crystal structure of the C2 fragment of streptococcal protein G in complex with the Fc domain of human IgG, *Structure.* 3 (1995) 265–278. doi:10.1016/S0969-2126(01)00157-5.
- [30] B.-K. Oh, Y.-K. Kim, Y.M. Bae, W.H. Lee, Detection of *Escherichia coli* O157:H7 Using Immunosensor Based on Surface Plasmon Resonance, *J. Microbiol. Biotechnol.* 12 (2002) 780–786.
- [31] M.B. Young, B.K. Oh, W. Lee, H.L. Won, J.W. Choi, Study on orientation of immunoglobulin G on protein G layer, *Biosens. Bioelectron.* 21 (2005) 103–110. doi:10.1016/j.bios.2004.09.003.
- [32] C. Diacci, M. Berto, M. Di Lauro, E. Bianchini, M. Pinti, D.T. Simon, F. Biscarini, C.A. Bortolotti, Label-free detection of interleukin-6 using electrolyte gated organic field effect transistors, *Biointerphases.* 12 (2017) 05F401. doi:10.1116/1.4997760.
- [33] J.M. Lee, H.K. Park, Y. Jung, J.K. Kim, S.O. Jung, B.H. Chung, Direct Immobilization of Protein G Variants with Various Numbers of Cysteine Residues on a Gold Surface, *Anal. Chem.* 79 (2007) 2680–2687. doi:10.1021/ac0619231.
- [34] M. Berto, C. Diacci, R. D'Agata, M. Pinti, E. Bianchini, M. Di Lauro, S. Casalini, A. Cossarizza, M. Berggren, D. Simon, G. Spoto, F. Biscarini, C.A. Bortolotti, M. Di Lauro, S. Casalini, A. Cossarizza, M. Berggren, D. Simon, G. Spoto, F. Biscarini, C.A. Bortolotti, EGOFET Peptide Aptasensor for Label-Free Detection of Inflammatory Cytokines in Complex Fluids, *Adv. Biosyst.* 2 (2018) 1700072. doi:10.1002/adbi.201700072.
- [35] T. Cramer, A. Campana, F. Leonardi, S. Casalini, A. Kyndiah, M. Murgia, F. Biscarini, Water-gated organic field effect transistors – opportunities for biochemical sensing and extracellular signal transduction, *J. Mater. Chem. B.* 1 (2013) 3728. doi:10.1039/c3tb20340a.
- [36] S.P. White, K.D. Dorfman, C.D. Frisbie, Operating and Sensing Mechanism of Electrolyte-Gated Transistors with Floating Gates: Building a Platform for Amplified Biodetection, *J. Phys. Chem. C.* 120 (2016) 108–117. doi:10.1021/acs.jpcc.5b10694.

- [37] M. Magliulo, A. Mallardi, M.Y. Mulla, S. Cotrone, B.R. Pistillo, P. Favia, I. Vikholm-Lundin, G. Palazzo, L. Torsi, Electrolyte-Gated Organic Field-Effect Transistor Sensors Based on Supported Biotinylated Phospholipid Bilayer, *Adv. Mater.* 25 (2013) 2090–2094. doi:10.1002/adma.201203587.
- [38] F.N. Ishikawa, M. Curreli, H.-K. Chang, P.-C. Chen, R. Zhang, R.J. Cote, M.E. Thompson, C. Zhou, A Calibration Method for Nanowire Biosensors to Suppress Device-to-Device Variation, *ACS Nano*. 3 (2009) 3969–3976. doi:10.1021/nn9011384.
- [39] J.L. Riechmann, S. Lain, J.A. Garcia, Highlights and prospects of potyvirus molecular biology, *J. Gen. Virol.* 73 (1992) 1–16. doi:10.1099/0022-1317-73-1-1.
- [40] P.H. Berger, P.J. Shiel, Potyvirus Isolation and RNA Extraction, in: *Plant Virol. Protoc.*, Humana Press, Totowa, NJ, 1998: pp. 151–160. doi:10.1385/0-89603-385-6:151.
- [41] S.M. Moghal, R.I.B. Francki, Towards a system for the identification and classification of potyviruses, *Virology*. 112 (1981) 210–216. doi:10.1016/0042-6822(81)90626-7.
- [42] A. Gustavo González, M. Ángeles Herrador, A practical guide to analytical method validation, including measurement uncertainty and accuracy profiles, *TrAC Trends Anal. Chem.* 26 (2007) 227–238. doi:10.1016/j.trac.2007.01.009.

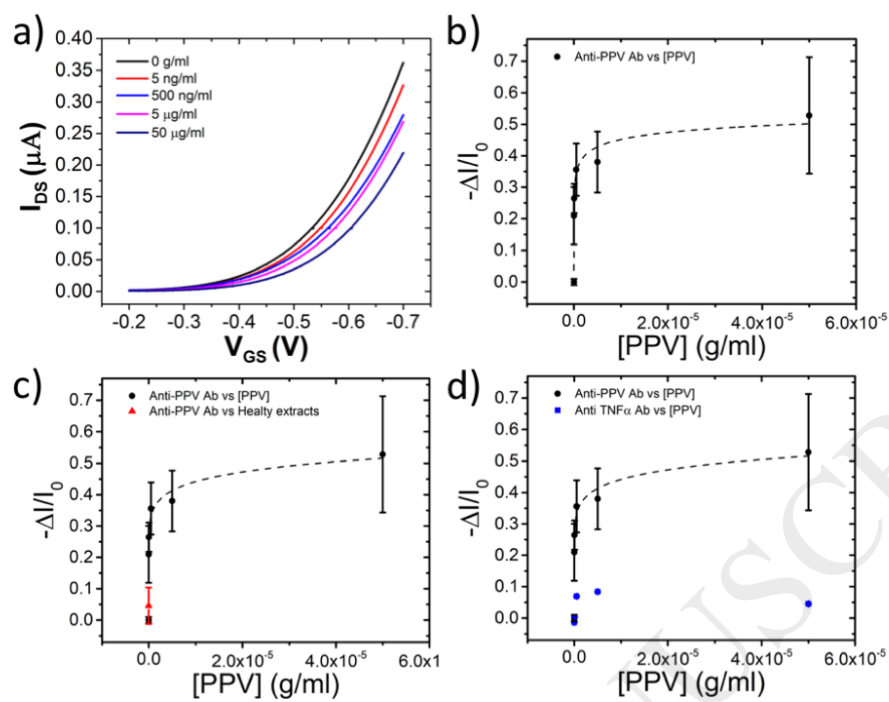
Figr-1



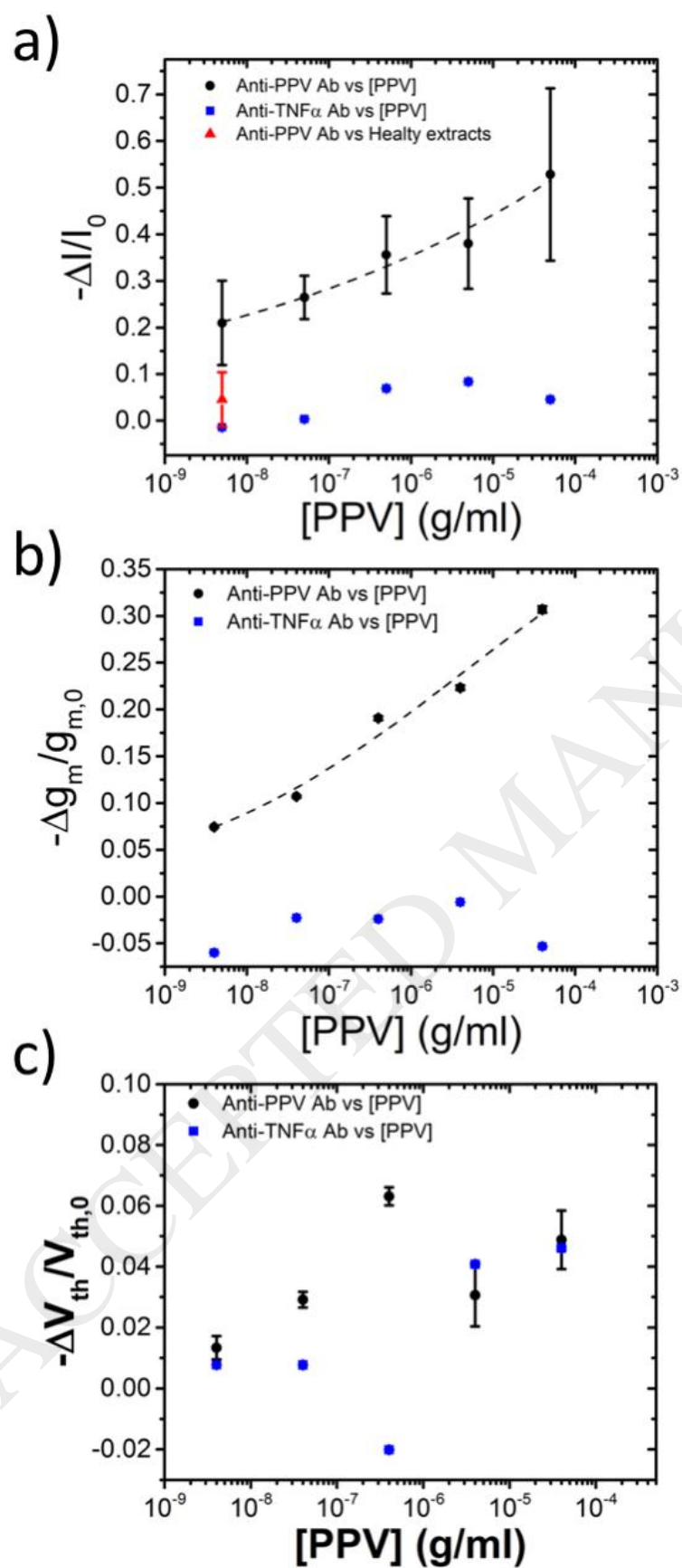
Figr-2



Figr-3



Figr-4



Figr-5

